Available online at www.sciencedirect.com
SCIENCE DIRECT®
Journal of Nuclear Materials 352 (2006) 144–150
journal of nuclear materials
www.elsevier.com/locate/jnucmat

Ab initio modeling of the behavior of helium and xenon in actinide dioxide nuclear fuels

M. Freyss *, N. Vergnet, T. Petit

CEA-Cadarache, DEN/DEC/SESC/LLCC, Bâtiment 151, 13108 Saint-Paul lez Durance cedex, France

Abstract

By means of an ab initio plane wave pseudopotential method, the behavior of helium in UO_2, PuO_2, AmO_2 and $(Am_{0.5}Pu_{0.5})O_2$ and of xenon in UO_2 is studied. We first show that a pseudopotential approach in the generalized gradient approximation (GGA) can satisfactorily describe the cohesive properties of these actinide dioxides. We then calculate the formation energies of point defects (vacancies and interstitials), as well as the incorporation and solution energies of helium in UO_2, PuO_2, AmO_2 and $(Am_{0.5}Pu_{0.5})O_2$, and of xenon in UO_2. The results are discussed according to the incorporation site of the gas atom in the fluorite lattice and according to the dioxide stoichiometry.

PACS: 61.72.Bd; 61.72.−y; 61.72.Ji

1. Introduction

The scope of this study is to shed light on the behavior of some rare gases in actinide oxides fuels: xenon in UO_2, and helium in UO_2, PuO_2, AmO_2 and $(Am,Pu)O_2$. Uranium-free actinide oxide compounds such as PuO_2, AmO_2 and $(Am,Pu)O_2$ are candidates as possible nuclear fuels in order to transmute long-lived minor actinides: long-lived radiotoxic elements, such as ^{239}Pu or ^{243}Am, could be separated from the standard UO_2 spent fuel and be then used in innovative oxide fuels in order to be transmuted into shorter life elements, reducing thus the radiotoxicity of the nuclear waste. Such actinide compounds have however a high alpha radioactivity producing a large amount of helium. This helium production, together with the production of fission gases like xenon, need a special attention because it could decrease the fuel performance. In particular, the presence of such rare gases can lead to the formation of bubbles and to a possible swelling of the material. This possible swelling could increase the pressure on the cladding of the fuel rod under irradiation and lead to its rupture. A similar risk exists for the containers of nuclear waste in storage conditions. The behavior of the fission gases and of helium is thus a key safety issue which has to be monitored in the standard UO_2 fuels as well as in the fuels envisioned for the future.

Using an ab initio approach, the behavior of helium and xenon is investigated here by first determining the formation energy of point defects, since vacancies constitute possible host sites for the

* Corresponding author. Tel.: +33 44 22 56 509; fax: +33 44 22 53 713.
E-mail address: Michel.Freyss@cea.fr (M. Freyss).

0022-3115/$ - see front matter © 2006 Elsevier B.V. All rights reserved.
doi:10.1016/j.jnucmat.2006.02.048

gaseous elements. The incorporation energy of the gaseous elements on different sites of the lattice is then calculated and the most favorable incorporation site is determined. The solubility of the gaseous elements is also evaluated.

The goal of this study is twofold. First, to compare the behavior of helium in different actinide dioxides (UO_2, PuO_2, AmO_2 and $(Am,Pu)O_2$). Second, to compare the behavior of two different rare gases (helium and xenon) in a given actinide dioxide (UO_2).

To this purpose, an ab initio pseudopotential plane-wave approach is used. It is particularly appropriate in order to perform the relaxation of the atomic positions around the defects and the gaseous elements. For uranium dioxide, similar studies of point defects and of the behavior of helium and fission gases were already performed [1–5] but using the local density approximation (LDA) for electronic exchange–correlation interactions. We use here the generalized gradient approximation (GGA) which was shown to give much better results for the cohesive properties of UO_2 [5] and of light actinides [6]. The non spin-polarized GGA however fails to reproduce the insulator character of actinide dioxides, but the cohesive properties calculated for bulk UO_2, PuO_2, AmO_2 and $(Am_{0.5}Pu_{0.5})O_2$ are nonetheless in good agreement with the experimental data, as shown in this study. A more accurate description of the 5f electron correlations and localized character in Pu and Am compounds would require the use of an approach beyond non spin-polarized LDA/GGA [7–11].

2. Method of calculation

In order to compute the ground-state properties of the systems considered, an ab initio plane wave pseudopotential method [12] based on the density functional theory (DFT) [13] is used. The electronic exchange–correlation interactions are taken into account in the generalized gradient approximation (GGA) [14]. Norm-conserving pseudopotentials for uranium, plutonium, americium, oxygen, xenon and helium were generated according to the Troullier–Martins scheme [15]. The actinide pseudopotentials were constructed considering the ionized (+2) configuration of the isolated atoms (zero occupancy of the 7s orbital) [6] and with the 6s 6p 6d 5f and 7s orbitals as valence orbitals. All calculations are performed using the ABINIT code [16] in the non spin-polarized scalar relativistic approximation. A 160 Ry energy cut-off in the expansion of the plane wave basis is used to calculate the cohesive properties of the bulk dioxides. All the compounds studied here have the fluorite structure (space group *Fm3m*). The mixed $(Am,Pu)O_2$ oxide is modeled with an equal amount of Pu and Am atoms in the cation sublattice of the fluorite structure, thus as a $(Am_{0.5}Pu_{0.5})O_2$ solid solution.

Point defects and gas incorporation are modeled in a supercell geometry. A 24 atom supercell is used for the study of helium in UO_2 and in $(Am_{0.5}Pu_{0.5})O_2$ and a 12 atom supercell is used for helium in PuO_2 and AmO_2 and for xenon in UO_2. In a previous study of point defects in UO_2 [5], it was shown that the formation energies agreed within 7% for a 12 atom and a 24 atom supercell. A similar agreement can be expected here for the incorporation energies of helium and xenon, which justifies that some calculations were performed with a 12 atom supercell only. A 120 Ry cut-off energy in the expansion of the plane wave basis is found to be enough to determine defect formation energies and incorporation energies with a 0.1 eV accuracy. The irreducible Brillouin zone is sampled by a $6 \times 6 \times 6$ Monkhorst–Pack grid [17].

3. Calculated bulk properties of actinide dioxides

The equilibrium lattice parameter, the bulk modulus and the cohesive energy of fluorite UO_2, PuO_2, AmO_2 and $(Am_{0.5}Pu_{0.5})O_2$ are calculated to show that the pseudopotential and the GGA approach used enables to satisfactorily describe those materials. Table 1 gives the results obtained, together with the comparison to experimental data. For UO_2, PuO_2 and AmO_2, the calculated structural and cohesive properties are in fair agreement with experiments. The relative errors are less than 1% for the lattice parameters. They are close to 20% for the cohesive energies, which is in the range of the usual errors that can be expected from ab initio calculations because of the poor description of the isolated atoms by the DFT–GGA. No reliable measurements of the bulk moduli of PuO_2 and AmO_2 exist but recent experiments enable to estimate their values to around 200 GPa [18], i.e. to values of the same order of magnitude as for other actinide dioxides (207 GPa for UO_2, 218 GPa for CmO_2) and also close to the values calculated here. For $(Am,Pu)O_2$ no experimental data could be found in the literature to compare our results. Further calculations (not shown in Table 1) for different

Table 1
Calculated equilibrium lattice parameter a, bulk modulus B and cohesive energy E_{CO} of fluorite UO_2, PuO_2, AmO_2 and $(Am_{0.5}Pu_{0.5})O_2$ and comparison to experimental data

Cohesive properties	Calculated	Experimental
UO_2	$a = 10.21$ a.u. $B = 195$ GPa $E_{CO} = 24.6$ eV	$a = 10.34$ a.u. $B = 207$ GPa $E_{CO} = 22.0$ eV
PuO_2	$a = 10.20$ a.u. $B = 197$ GPa $E_{CO} = 24.0$ eV	$a = 10.20$ a.u $B \sim 200$ GPa [18] $E_{CO} = 19.7$ eV
AmO_2	$a = 10.16$ a.u. $B = 196$ GPa $E_{CO} = 22.7$ eV	$a = 10.19$ a.u. $B \sim 200$ GPa [18] $E_{CO} = 17.8$ eV
$(Am_{0.5}Pu_{0.5})O_2$	$a = 10.19$ a.u. $B = 197$ GPa $E_{CO} = 18.02$ eV	/

Am/Pu ratios (25, 50 and 75 at.%) in (Am,Pu)O_2 show that the lattice parameter of this compound follows the Vegard's law.

4. Stability of point defects in UO_2, PuO_2, AmO_2 and $(Am_{0.5}\ Pu_{0.5})O_2$

The stability in the fluorite lattice of different types of point defects is studied: vacancies, interstitials at the octahedral site, Frenkel pairs and Schottky defects.

The formation energies $E^F_{V_X}$ and $E^F_{I_X}$ of a vacancy (V_X) and an interstitial (I_X) of the X specie are obtained from the total energies of the system at constant volume with and without the defect, according to $E^F_{V_X} = E^{N-1}_{V_X} - E^N + E_X$, and $E^F_{I_X} = E^{N+1}_{I_X} - E^N - E_X$, where $E^{N-1}_{V_X}$ and $E^{N+1}_{I_X}$ are the calculated total energies of the supercell with the defects, E^N is the calculated total energy of the supercell without defect and containing N atoms, and E_X is the calculated energy of the X element in the chosen reference state (the metallic bulk crystal for actinide defects and a O_2 molecule for oxygen defects).

Frenkel pairs consist of a non-interacting vacancy and an interstitial of the same chemical element. The formation energy of a Frenkel pair of the X specie ($E^F_{FP_X}$) is thus given by $E^F_{FP_X} = E^{N-1}_{V_X} + E^{N+1}_{I_X} - 2E^N$.

A Schottky defect is a more complex defect consisting of an actinide vacancy and two oxygen vacancies, all of which are again supposed to be non-interacting. The formation energy of a Schottky defect (E^F_S) is given by $E^F_S = E^{N-1}_{V_{An}} + 2E^{N-1}_{V_O} - 3\frac{N-1}{N}E^N$.

The calculated formation energies of point defects in UO_2, PuO_2, AmO_2 and $(Am_{0.5}Pu_{0.5})O_2$ are given in Table 2 for oxygen and actinide vacancies, interstitials at the octahedral site, Frenkel pairs, and Schottky defects. The formation energies are obtained after performing the relaxation of the atomic positions in the supercell at constant volume. The values for UO_2 are taken from Ref. [5].

Table 2 shows that the formation energies in PuO_2, AmO_2 and $(Am_{0.5}Pu_{0.5})O_2$ follow the same trends. However, an interesting point shown is that the formation energies of oxygen interstitials are positive, although small, in both PuO_2 and AmO_2. This was also found by Petit et al. [10] for PuO_2 using a more appropriate approach to treat the localized character of the 5f electrons. Oxygen incorporation in PuO_2 and AmO_2 thus contrasts to oxygen incorporation in UO_2: the formation energy of an oxygen interstitial in UO_2 is found negative (−2.5 eV) [5], in agreement with the well known first step of oxidation of UO_2 occurring by oxygen incorporation at an interstitial site. A different oxidation mechanism in PuO_2 and AmO_2 compared to UO_2 is thus expected. Oxidation experiments of PuO_2 conducted by Martin et al. [19] revealed that hyper-stoichiometric PuO_{2+x} is indeed difficult to obtain. The oxidation of PuO_2 might only occur under very specific conditions, possibly involving hydrolysis, as discussed from the reaction energies obtained by ab initio calculations by Khorzhavyi et al. [11].

Table 2
Calculated formation energies of point defects in UO_2 [5], PuO_2, AmO_2 and $(Am_{0.5}Pu_{0.5})O_2$: oxygen and actinide vacancies (V_O and V_{An}), interstitials (I_O and I_{An}), Frenkel pairs (FP_O and FP_{An}), and Schottky defects (S). In $(Am_{0.5}Pu_{0.5})O_2$, the formation energies of both a Pu vacancy and a Am vacancy are reported

E^F (eV)	V_O	I_O	V_{An}	I_{An}	FP_O	FP_{An}	S
UO_2	6.1	−2.5	4.8	7.0	3.6	11.8	5.6
PuO_2	5.3	0.1	9.2	4.9	5.3	14.1	9.1
AmO_2	3.7	1.4	11.9	4.7	5.1	16.6	8.4
$(Am_{0.5}Pu_{0.5})O_2$	4.2	/	11.9 (Pu) 11.0 (Am)	/	/	/	/

5. Incorporation of xenon in UO_2 and of helium in UO_2, PuO_2, AmO_2 and $(Am_{0.5}Pu_{0.5})O_2$

5.1. Incorporation energies

The incorporation energy E_{inc} is defined as the energy required to incorporate an helium (or a xenon) atom at a pre-existing vacancy or at an interstitial site: $E_{inc} = E_{He}^{N,N+1} - E^{N-1,N} - E_{He}$, where $E_{He}^{N,N+1}$ is the energy of the supercell with an incorporated helium atom, $E^{N-1,N}$ is the energy of the supercell with the empty trap site, and E_{He} is the energy of an isolated helium atom. A negative incorporation energy is indicative of the stability of the incorporated element in the lattice. The incorporation energies are calculated taking into account the relaxation of the atomic positions in the supercell at constant volume, and for different incorporation sites: a cation site (An), an oxygen site (O) and an octahedral interstitial site (Int.). The incorporation energies obtained for helium in UO_2, PuO_2, AmO_2 and $(Am_{0.5}Pu_{0.5})O_2$ are reported in Table 3, and those for xenon in UO_2 in Table 4.

Helium incorporation shows the same trend in all the actinide dioxides considered: the incorporation energies are very small, hardly larger than 1 eV. The sign of the incorporation energies however varies according to the dioxide considered. It is found negative only in UO_2 at an interstitial site (confirming the localization measurements by Nuclear Reaction Analysis by Garrido et al. [20]) and in PuO_2 at an oxygen site. In AmO_2 and $(Am_{0.5}Pu_{0.5})O_2$ the incorporation energies are always positive, the smallest values being obtained for incorporation at an actinide site.

The xenon incorporation energy, calculated only for UO_2, shows a clearer and much different picture (see Table 4): the energies are positive and of the order of 10 eV, whatever the incorporation site, indicating that diluted xenon is strongly unstable in the UO_2 lattice. A similar behavior of xenon can be expected in other actinide dioxides.

Table 3
Calculated incorporation energies of helium in UO_2, PuO_2, AmO_2 and $(Am_{0.5}Pu_{0.5})O_2$ on different sites of the fluorite lattice: the actinide site (An), the oxygen site (O) and the octahedral interstitial site (Int). In $(Am_{0.5}Pu_{0.5})O_2$, the incorporation energy is calculated at both a Pu site and a Am site

E_{inc} (eV)	He (An)	He (O)	He (Int.)
UO_2	0.4	2.4	−0.1
PuO_2	0.7	−0.5	0.4
AmO_2	0.4	0.5	1.1
$(Am_{0.5}Pu_{0.5})O_2$	0.1 (Pu) 0.2 (Am)	0.8	0.7

Table 4
Calculated incorporation energies of xenon in UO_2 on different sites of the fluorite lattice: the uranium site (U), the oxygen site (O) and the interstitial site (Int)

E_{inc} (eV)	Xe (U)	Xe (O)	Xe (Int.)
UO_2	13.9	9.4	11.2

5.2. Modification of the volume induced by the incorporation of the gaseous elements

Besides the incorporation energies, the volume modifications of the supercell induced by helium and xenon incorporation are also calculated here. This enables to estimate the potential swelling of the crystal in the presence of diluted helium and xenon atoms. The relaxation of the supercell volume is performed by minimizing the internal pressure of the solid, with the helium or xenon atoms incorporated in the three different sites considered. Table 5 gives the results obtained for the absolute variations ΔV of the supercell volume and the variations $\Delta V/V_0$ relative to the unit cell volume V_0 of UO_2, PuO_2 or AmO_2. This latter quantity, rather than the volume variation relative to the defect free supercell volume V, enables to compare the results obtained with supercells of different sizes [5], and is representative of the swelling of the crystal induced by the incorporation of the gaseous elements. For helium incorporation in UO_2, PuO_2 and AmO_2, the maximum relative increase of the

Table 5
Volume variation induced by helium incorporation in UO_2, PuO_2 and AmO_2, and by xenon incorporation in UO_2: absolute volume variation ΔV (a.u.^{3}) and variation $\Delta V/V_0$ (%) relative to the elementary volume of UO_2, PuO_2 or AmO_2. The results are given for the different incorporation sites: the actinide substitution site (An), the oxygen site (O) and the octahedral interstitial site (Int)

Volume variation		An	O	Int
He in UO_2	ΔV (a.u.^{3})	−74	37	36
	$\Delta V/V_0$ (%)	−27%	14%	14%
He in PuO_2	ΔV (a.u.^{3})	−104	38	19
	$\Delta V/V_0$ (%)	−39%	14%	7%
He in AmO_2	ΔV (a.u.^{3})	−86	53	13
	$\Delta V/V_0$ (%)	−33%	20%	5%
Xe in UO_2	ΔV (a.u.^{3})	110	208	180
	$\Delta V/V_0$ (%)	41%	78%	68%

volume do not exceed 20% (20% in AmO_2, and 14% in both UO_2 and PuO_2). The incorporation of helium in an actinide site induces a decrease of the supercell volume of around 30–40%. On the other hand, xenon in UO_2 induces a large swelling of the supercell of around 78% at its most favorable incorporation site (oxygen site). This is related to the larger atomic radius of this element compared to oxygen. Xenon incorporation at the uranium site induces a 41% swelling of the supercell, and 68% at the interstitial site.

6. Solubility of helium and xenon

The incorporation energy as defined above does not take into account any thermodynamic equilibrium between the different trap sites. This means that even though the incorporation energy at a given trap site is the lowest, if the concentration of this trap is very small, the gas atom is unlikely to be actually soluble. It is therefore required to take into account the concentration of the trap sites in the discussion of the solubility of the gas atoms. This is done by defining the solution energy.

The solution energy E_{sol} is defined by $E_{sol} = E_{inc} + E_{Vac}^{Fapp}$, where E_{inc} is the incorporation energy as calculated in the previous section, and E_{Vac}^{Fapp} is the apparent formation energy of the trap at which the gaseous element is incorporated (see also Refs. [3,4]). The apparent formation energy depends on the vacancy concentration as $E_{Vac}^{Fapp} = -kT\ln([v_X])$. It is possible to calculate the variation of the vacancy concentrations $[v_X]$ as a function of the stoichiometry x in $AnO_{2\pm x}$ (with An = U, Pu, Am and $(Am_{0.5}Pu_{0.5})$) with the so-called Point Defect Model [21,22]. This model links the point defect concentrations to both the formation energies of defects and the deviation from stoichiometry x:

$$[v_O]\cdot[i_O] = \exp\left(-\frac{E^F_{FP_O}}{k_BT}\right) \quad [v_{An}]\cdot[i_{An}] = \exp\left(-\frac{E^F_{FP_{An}}}{k_BT}\right)$$

$$[v_O]^2\cdot[i_{An}] = \exp\left(-\frac{E^F_S}{k_BT}\right)$$

$$2\cdot[v_{An}] + [i_O] = 2\cdot[i_{An}] + 2\cdot[v_O] + x$$

where $E^F_{FP_O}$, $E^F_{FP_{An}}$, and E^F_S are respectively the formation energies of oxygen Frenkel pairs, actinide Frenkel pairs, and Schottky defects, and where $[v_X]$ and $[i_X]$ are the vacancy and interstitial concentrations. T is an arbitrary temperature, which was fixed here at 1700 K. By solving this set of equations using the formation energies previously calculated (Table 2), the evolution of the solution energy as a function of the deviation from stoichiometry x can be calculated. For $(Am_{0.5}Pu_{0.5})O_2$, since the formation energies of interstitials were not calculated, we assume that the formation energies of Frenkel pairs and Schottky defects are the average values of the formation energies of the corresponding defects in AmO_2 and in PuO_2 (see Table 2).

As an example, the variations of the solution energy of helium in UO_2 are plotted in Fig. 1 as a function of the stoichiometry x and for the three different incorporation sites. Helium is found soluble in UO_2 whatever the stoichiometry because of the negative incorporation energy of helium at the interstitial site. The solution energy, which in the case of the interstitial site equals the incorporation energy, amounts to −0.1 eV. This very small value places however helium rather at the edge of solubility, with a probable competition between bubble formation and re-solubility. The previous calculations of the helium behavior in UO_2 by Crocombette [4] using the LDA approximation also predicted small solution energies for He, but a negative value only for the hyperstoichiometric dioxide. Moreover, contrary to the GGA used here, the LDA could not predict the octahedral interstitial site as the stable incorporation site of He.

For PuO_2, the solution energy is found negative for helium incorporation at an oxygen site. How surprising this result may be, it can be related to the small but negative incorporation energy found for helium at an oxygen vacancy and to the rapidly increasing concentration of oxygen vacancies with x in hypostoichiometric PuO_2. The solution energy is

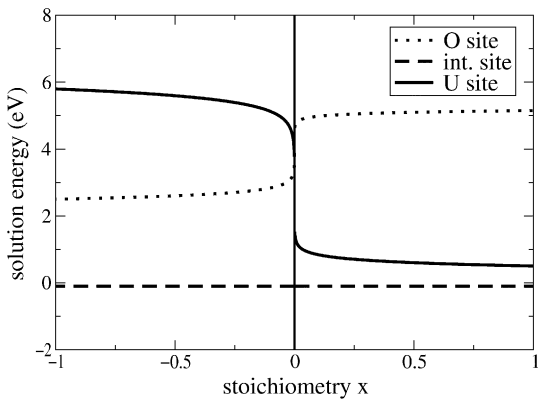

Fig. 1. Solution energy (eV) of helium in UO_{2+x} as a function of the stoichiometry (−) x and for the different incorporation sites: the oxygen site (dotted curve), the uranium site (solid curve), and the octahedral interstitial site (dashed line).

however very small (less than half an eV). For stoichiometric and hyperstoichiometric PuO_2, helium is found not soluble: the smallest values for the solution energy is found in both cases for an interstitial site. The solution energies are again small.

In AmO_2 and $(Am_{0.5}Pu_{0.5})O_2$, as well, small values (less than 1 eV) for the helium solution energy are obtained. But contrary to PuO_2, the solution energies are found positive whatever the stoichiometry of the oxides and whatever the incorporation site of helium.

Finally, for xenon in UO_2, from the much larger incorporation energies it results solution energies of the order of 10 eV as well. Diluted xenon in the UO_2 lattice is thus clearly not soluble whatever the incorporation site and the stoichiometry. The precipitation of xenon into bubbles or clusters is thus certainly more favorable. The formation of such xenon aggregates has been indeed recently evidenced by ion-implantation experiments by Garcia et al. [23].

7. Conclusion

In this study, we first show that the ab initio pseudopotential method in the generalized gradient approximation (GGA) gives satisfactory results for the lattice parameter, the bulk modulus and the cohesive energy of uranium, plutonium and americium dioxides.

The calculation of the formation energies of point defects in PuO_2 and AmO_2 confirms that these materials probably have an oxidation mechanism different to the one of UO_2, since an oxygen interstitial at the octahedral site is not found stable in PuO_2 and AmO_2, unlike in UO_2.

To study the behavior of helium in UO_2, PuO_2, AmO_2 and $(Am_{0.5}Pu_{0.5})O_2$, and of xenon in UO_2, the incorporation energy and the solution energy of these elements were calculated. A negative solution energy, indicative of solubility, is found for helium in UO_2 for all stoichiometries and in hypostoichimetric PuO_2. On the other hand, in AmO_2 and in $(Am_{0.5}Pu_{0.5})O_2$, a positive helium solution energy is obtained whatever the stoichiometry and the incorporation site of the helium atom. The estimation of the helium solubility in the different actinide dioxides shows the same trend: the small values obtained for the helium solution energies (of the order of 1 eV or less) in UO_2, PuO_2, AmO_2 and $(Am_{0.5}Pu_{0.5})O_2$ makes it difficult to conclude on the stability of helium in a diluted form or as bubbles. Helium appears at the edge of solubility and a competition between bubble precipitation and re-solubility can be expected in all actinide dioxides considered here. A clearer and much different picture compared to helium is found for xenon in UO_2, for which large positive incorporation and solution energies are obtained, indicative of the non solubility of xenon in UO_2. A similar behavior can be expected for xenon in the other actinide dioxides, although it was not explicitly studied here.We finally emphasize that we could so far only consider diluted gas atoms here, the ab initio study of bubble stability is still out of reach with the computer resources currently at hand.

Acknowledgements

We wish to thank J.P. Crocombette, F. Jollet and S. Bernard for fruitful discussions. The European Commission is acknowledged for its financial support through the FUTURE (Fuel for Transmutation of Transuranium Elements) project. The study of point defects in actinide oxides and of the behavior of helium in UO_2 is done in the framework of the ACTINET Network of Excellence.

References

[1] T. Petit, G. Jomard, C. Lemaignan, B. Bigot, A. Pasturel, J. Nucl. Mater. 275 (1999) 119.
[2] T. Petit, M. Freyss, P. Garcia, P. Martin, M. Ripert, J.P. Crocombette, F. Jollet, J. Nucl. Mater. 320 (2003) 133.
[3] J.P. Crocombette, F. Jollet, L. Thien Nga, T. Petit, Phys. Rev. B 64 (2001) 104107.
[4] J.P. Crocombette, J. Nucl. Mater. 305 (2002) 29.
[5] M. Freyss, J.P. Crocombette, T. Petit, J. Nucl. Mater. 347 (2005) 44.
[6] N. Richard, S. Bernard, F. Jollet, M. Torrent, Phys. Rev. B 66 (2002) 235112.
[7] A.L. Kutepov, S.G. Kutepova, J. Phys.: Condens. Matter. 15 (2003) 2607.
[8] S.Y. Savrasov, G. Kotliar, Phys. Rev. Lett. 84 (2000) 3670.
[9] S.Y. Savrasov, G. Kotliar, E. Abrahams, Nature 401 (2001) 793.
[10] L. Petit, A. Svane, Z. Szotek, W.M. Temmerman, Science 301 (2003) 498.
[11] P.A. Korzhavyi, L. Vitos, D.A. Andersson, B. Johansson, Nature Mater. 3 (2004) 225.
[12] M.C. Payne, M.P. Teter, D.C. Allan, T.A. Arias, J.D. Joannopoulos, Rev. Mod. Phys. 64 (1992) 1045.
[13] P. Hohenberg, W. Kohn, Phys. Rev. 136 (1964) B864; W. Kohn, L.J. Sham, Phys. Rev. 140 (1965) A1133.
[14] J.P. Perdew, K. Burke, M. Ernzerhof, Phys. Rev. Lett. 77 (1996) 3865.
[15] N. Troullier, J.L. Martins, Phys. Rev. B 43 (1991) 1993.

[16] X. Gonze et al., Comput. Mater. Sci. 25 (2002) 478. Available from: <http://www.abinit.org> .
[17] H.J. Monkhorst, J.D. Pack, Phys. Rev. B 13 (1976) 5188.
[18] G.H. Lander, M. Idiri, private communication.
[19] P. Martin, S. Grandjean, M. Ripert, M. Freyss, P. Blanc, T. Petit, J. Nucl. Mater. 320 (2003) 138.
[20] F. Garrido, L. Nowicki, G. Sattonnay, T. Sauvage, L. Thomé, Nucl. Instr. and Meth. B 219–220 (2004) 196.
[21] Hj. Matzke, J. Chem. Soc. Faraday Trans. II 83 (1987) 1121.
[22] A.B. Lidiard, J. Nucl. Mater. 19 (1966) 106.
[23] P. Garcia, P. Martin, G. Carlot, E. Castelier, M. Ripert, C. Sabathier, C. Valot, F. D'Acapito, J.-L. Hazemann, O. Proux, V. Nassif, J. Nucl. Mater., these proceedings, doi:10.1016/j.jnucmat.2006.02.047.